

# Complex Dynamics of Correlated Electrons in Molecular Double Ionization by an Ultrashort Intense Laser Pulse

J. Liu,<sup>1</sup> D.F. Ye,<sup>1</sup> J. Chen,<sup>1</sup> and X. Liu<sup>2</sup>

<sup>1</sup>*Institute of Applied Physics and Computational Mathematics, P.O.Box 100088, Beijing, P. R. China*

<sup>2</sup>*State Key Laboratory of Magnetic Resonance and Atomic and Molecular Physics, Wuhan Institute of Physics and Mathematics, Chinese Academy of Sciences, Wuhan 430071, P. R. China*

With a semiclassical quasi-static model we achieve an insight into the complex dynamics of two correlated electrons under the combined influence of a two-center Coulomb potential and an intense laser field. The model calculation is able to reproduce experimental data of nitrogen molecules for a wide range of laser intensities from tunnelling to over-the-barrier regime, and predicts a significant alignment effect on the ratio of double over single ion yield. The classical trajectory analysis allows to unveil sub-cycle molecular double ionization dynamics.

PACS numbers: 33.80.Rv, 34.80.Gs, 42.50.Hz

Within the strong-field physics community, there has been increasing interest on double ionization (DI) of molecules in intense laser pulses and a large variety of novel phenomena has emerged. The diatomic molecules show a much higher double ionization yield than the prediction of the single-active-electron (SAE) model by many orders of magnitude [1, 2], and DI yield as well as ionized-electron momentum distribution exhibit a strong dependence on molecular structure and alignment [3, 4, 5]. Experimental data indicate that a rescattering mechanism is responsible for nonsequential double ionization (NSDI) caused by strong correlation between two electrons. In this process, which has been extensively investigated for atoms [6], an electron freed by tunnelling ionization is driven by the laser electric field into a recollision with its parent ion. This essentially classical rescattering picture implicitly suggests that the well synchronized recolliding electron burst with respect to the laser field be an alternative attosecond pulse source for the probe of molecular dynamics [7]. However the details of this pivotal recolliding event for molecules remain unknown.

The complexity of the dynamics of the two correlated electrons responding to a two-center nuclear attraction and the laser force, on the other hand, poses a great challenge to any theoretical treatment. For instance, a time-dependent, three-dimensional quantum mechanical computation from first principles has not yet been accomplished even for the simpler case of atoms [8]. This leaves approximate approaches developed recently, such as one-dimensional quantum model [9], many-body S-matrix [10] and simplified classical methods [11]. However, the complex electron dynamics which is crucial for molecular DI is still not fully explored and the theoretical results can not account for experimental data quantitatively. In this letter, we employ a feasible semiclassical theory, i.e. an *ab initio* 3D calculation including classical rescattering and quantum tunnelling effects, providing an intuitive way of understanding the complex dynamics involved in the molecular DI. Our calculation is capable of reproducing unusual excess DI rate for a wide range of

laser intensities quantitatively (see Fig. 1), thus consolidating the classical rescattering view of molecular DI. In particular, with classical trajectory analysis, we are able to unveil the sub-cycle dynamics behind molecular DI and predict a significant influence of molecular alignment on the ratio of double over single ion yield.

The model we propose here is in the spirit of that of semiclassical treatment of DI of atoms in high-intensity field [12]. We consider a molecule composed of two nucleus and two valence electrons interacting with an infrared laser pulse. When the laser intensity is smaller than a threshold value (see Fig. 1), one electron is released at the outer edge of the suppressed Coulomb potential through quantum tunnelling (Fig. 2(a)) with a rate  $\varpi(t_0)$  given by molecular ADK formula [13]. The initial position of the tunnelled electron can be de-

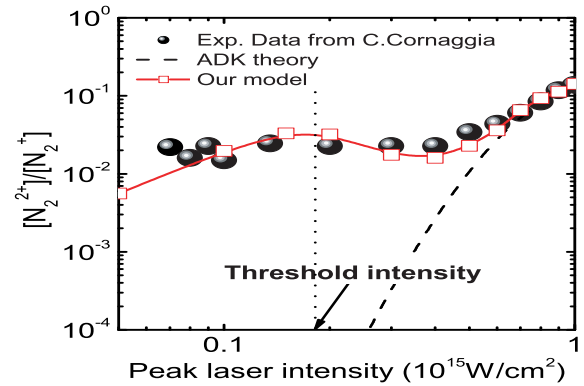


FIG. 1: (color online). Comparison between DI data [2] and theory for nitrogen molecule.  $0.185 \text{ PW/cm}^2$  is the threshold intensity separates the tunnelling and over-the-barrier regime as schematically plotted in Fig. 2. In the calculation, the laser frequency  $\omega$  of  $0.05695 a.u.$  and the number of optical cycle of 37 are chosen to match the experiments of Cornaggia [2]. To our knowledge, the results from our calculations are the first to be in good agreement with experimental data for a wide range of laser intensities from tunnelling to over-the-barrier regime.

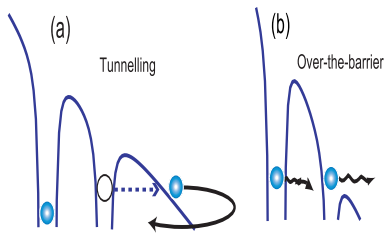


FIG. 2: (color online). Schematic representation of the ionization mechanisms addressed in this work. (a) Tunnelling ionization. (b) Over-the-barrier ionization.

rived from the equation,  $-\frac{1}{r_{a1}} - \frac{1}{r_{b1}} + \int \frac{|\Psi(\mathbf{r}')|^2}{|\mathbf{r}_1 - \mathbf{r}'|^r} d\mathbf{r}' + I_{p1} - z_1\varepsilon(t_0) = 0$  with  $x_1 = y_1 = 0$ . The wavefunction  $\Psi$  is given by the linear combination of the atomic orbital-molecular orbital (LCAO-MO) approximation [14]. The initial velocity of tunnelled electron is set to be  $(v_\perp \cos \varphi, v_\perp \sin \varphi, 0)$ , where  $v_\perp$  is the quantum-mechanical transverse velocity distribution satisfying  $w(v_\perp)dv_\perp = \frac{2(2I_{p1})^{1/2}v_\perp}{\varepsilon(t_0)} \exp(-\frac{v_\perp^2(2I_{p1})^{1/2}}{\varepsilon(t_0)})dv_\perp$ , and  $\varphi$  is the polar angle of the transverse velocity uniformly distributed in the interval  $[0, 2\pi]$  [12]. For the bound electron, the initial position and momentum are depicted by single-electron microcanonical distribution (SMD) [15],  $F(\mathbf{r}_2, \mathbf{p}_2) = k\delta[I_{p2} - \mathbf{p}_2^2/2 - W(r_{a2}, r_{b2})]$ , where  $k$  is the normalization factor,  $I_{p2}$  denotes the ionization energy of molecular ions, and  $W(r_{a2}, r_{b2}) = -1/r_{a2} - 1/r_{b2}$  is the total interaction potential between the bound electron and two nuclei.

The above scheme is only applicable when the laser intensity is lower than the threshold value [14]. To give a complete description of the DI of molecular system for the whole range of the laser intensities (see Fig. 1), one needs to extend the above model to the over-the-barrier regime (Fig. 2b). This is done by constructing the initial conditions with double-electron microcanonical distribution (DMD) [16], i.e.,  $F(\mathbf{r}_1, \mathbf{r}_2, \mathbf{p}_1, \mathbf{p}_2) = \frac{1}{2}[f_\alpha(\mathbf{r}_1, \mathbf{p}_1)f_\beta(\mathbf{r}_2, \mathbf{p}_2) + f_\beta(\mathbf{r}_1, \mathbf{p}_1)f_\alpha(\mathbf{r}_2, \mathbf{p}_2)]$ , with  $f_{\alpha,\beta}(\mathbf{r}, \mathbf{p}) = k\delta[I_{p1} - \frac{\mathbf{p}^2}{2} - W(r_a, r_b) - V_{\alpha,\beta}(\mathbf{r})]$ , where  $V_{\alpha,\beta}(\mathbf{r}) = \frac{1}{r_{b,a}}[1 - (1 + \kappa r_{b,a})e^{-2\kappa r_{b,a}}]$  represents the mean interaction between the electrons,  $\kappa$  can be obtained by a variational calculation of the ionization energy of molecules.

The subsequent evolution of the two-electron system with the above initial conditions is simulated by the classical Newtonian equations of motion:  $\frac{d^2\mathbf{r}_i}{dt^2} = \varepsilon(t) - \nabla(V_{ne}^i + V_{ee})$ . Here index  $i$  denotes the two different electrons,  $V_{ne}^i$  and  $V_{ee}$  are Coulomb interaction between nuclei and electrons and between two electrons, respectively.  $V_{ne}^i = -\frac{1}{r_{ai}} - \frac{1}{r_{bi}}$ ,  $V_{ee} = \frac{1}{|\mathbf{r}_1 - \mathbf{r}_2|}$ , where  $r_{ai}$  and  $r_{bi}$  are distances between the  $i$ th electron and nucleus  $a$  and  $b$ . The above Newtonian equations of motion are solved using the 4-5th Runge-Kutta algorithm and DI events are identified by energy criterion. In our calcula-

tions, more than  $10^5$  weighted (i.e., by rate  $\varpi(t_0)$ ) classical two-electron trajectories are traced and a few thousands or more of DI events are collected for statistics. Convergence of the numerical results is further tested by increasing the number of launched trajectories twice.

The above model is applied to the study on DI of molecular nitrogen. We first calculate the ratio between the double and single ionization yield with respect to the peak laser intensities from  $5 \times 10^{13} \text{W/cm}^2$  to  $1 \times 10^{15} \text{W/cm}^2$ . In Fig. 1 the calculated results are compared with that of recent experiments of Cornaggia *et.al.* [2] and a good agreement is obtained for such a broad range of laser intensities.

In the following, we proceed to explore the correlated electron dynamics responsible for DI of molecular nitrogen. The classical trajectory method allows us to select out the individual DI trajectories and back analyze their dynamics in detail. The typical electron trajectories are shown in Fig. 3, presented in an energy versus time plot. The threshold value of  $0.185 \text{PW/cm}^2$  separates the DI data into two parts. When the peak laser intensity is below this value, there exist two dominant processes responsible for emitting both electrons, namely, collision-ionization (CI) and collision-excitation-ionization (CEI), as shown in Fig. 3(a)(b), respectively. For CI, the tunnelled electron is driven back by the oscillating laser field to collide with the bound electron near its parent ion causing an instant ( $\sim$  attosecond) ionization. For CEI, DI event is created by recollision with electron impact excitation followed by a time-delayed ( $\sim$  a few optical periods) field ionization of the excited state. When the laser intensity is above the threshold value, over-the-barrier ionization emerges. In this regime we observe more complicated trajectories for DI processes. Except for CI (Fig. 3(c)) and CEI (Fig. 3(d)) trajectories similar to tunnelling case, there are multiple-collision trajectories as shown in Fig. 3(e),(f) as well as collisionless trajectory of Fig. 3(g). In Fig. 3(e) and (f), initially two valence electrons entangle each other, experience a multiple-collision and then emit. The four types of trajectories shown in Fig. 3(c-f) represent the dominant processes of DI in the plateau regime from  $0.185 \text{PW/cm}^2$  to  $0.5 \text{PW/cm}^2$ , each of them accompanied by one or multiple times of collisions between two electrons [17, 18, 19]. However, above  $0.5 \text{PW/cm}^2$ , DI is dominated by a collisionless sequential ionization whose typical trajectory is represented by Fig. 3(g). In this regime results from our model agree with ADK theory.

The analysis of trajectories of electron-electron pairs may provide insight into the complicated dynamics of DI with sub-cycle time resolution, and the important information is revealed by the laser field phase at the moments of collision and ionization [20, 21]. We choose three typical laser intensities,  $0.12 \text{PW/cm}^2$ ,  $0.4 \text{PW/cm}^2$  and  $1 \text{PW/cm}^2$ , representing the tunnelling, plateau and sequential ionization regime, respectively.

Fig. 4(a) shows the diagram of DI yield versus laser phase at the moment of closest collision. In the tun-

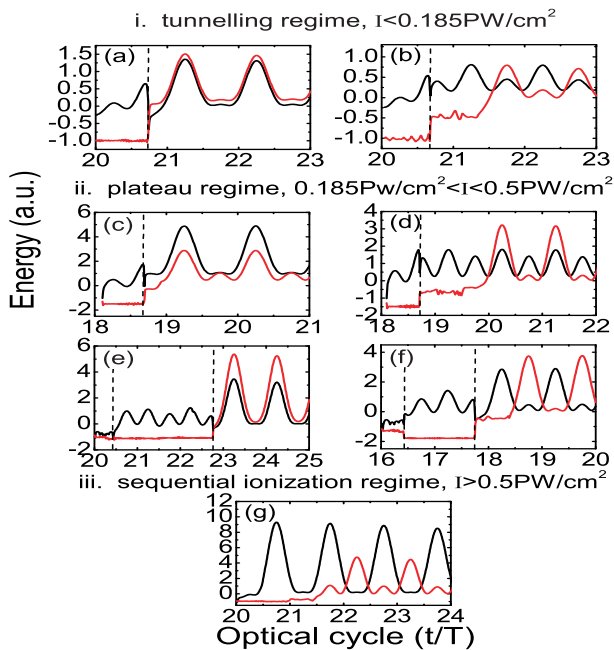


FIG. 3: (color online). Typical energy evolution of the electron pair in different laser intensity regime. Vertical dashed lines indicate the moment when collision between electrons emerge.

nelling regime (i.e.,  $0.12 \text{PW}/\text{cm}^2$ ), we note that the collision can occur throughout most of the laser cycle and the peak emerges slightly before the zeroes of the laser field. This is consistent with the prediction of simple-man model [22] and recent results from purely classical calculation [23]. However, for the other two cases, the collision between the two correlated electrons occurs mainly at peak laser field. This is because the ionization mechanism changes at the transition to over-the-barrier regime, where both electrons rotate around the nuclei and their distance could be very close before one of them is driven away by the external field.

Fig. 4(b) plots DI yield as a function of the laser phase at the instant of ionization. Most DI occurs around the maximum of laser field for different intensity regime. Interestingly, for the tunnelling case, we observe a peak shift of  $\sim 30^\circ$  off the field maximum. With assuming that the colliding electron leaves the atom with no significant energy and electron-electron momentum exchange in final state is negligible [24], the parallel momentum  $k_{1,2}^{\parallel}$  of each electron results exclusively from the acceleration in the optical field:  $k_{1,2}^{\parallel} = \pm 2\sqrt{U_p} \sin \omega t_{ion}$  [21]. The above shifted peak indicates the accumulation of the emitted electrons at  $k_1^{\parallel} = k_2^{\parallel} = \pm \sqrt{U_p}$  in the first and third quadrants of parallel momentum plane  $(k_1^{\parallel}, k_2^{\parallel})$ . It is consistent with the experimental data of Ref. [5] (see their Fig. 2).

Fig. 4(c) shows the phase angle of momentum vector

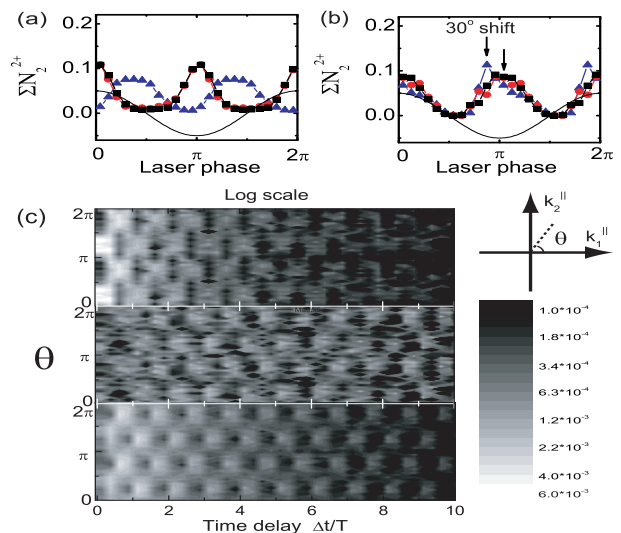


FIG. 4: (color online). DI yield vs laser phase when (a) the two electrons become closest; (b) both the electrons are ionized, at different laser intensity  $0.12 \text{PW}/\text{cm}^2$  (triangle),  $0.4 \text{PW}/\text{cm}^2$  (circle) and  $1 \text{PW}/\text{cm}^2$  (square), respectively. (c) The relationship between the correlated momentum and the delay time at  $0.12 \text{PW}/\text{cm}^2$  (upper),  $0.4 \text{PW}/\text{cm}^2$  (mid) and  $1.0 \text{PW}/\text{cm}^2$  (low), respectively.

$(k_1^{\parallel}, k_2^{\parallel})$  with respect to the delayed time between the closest collision and ionization. The integration over the phase angle gives total DI yield versus the delayed time. In all three cases we observe a long-tail up to several optical periods. For the sequential ionization of  $1 \text{PW}/\text{cm}^2$ , it means that the second electron is slowly (i.e., waiting for a few optical cycles) ionized after the first electron is deprived from nuclei by the laser field. In the tunnelling regime, the long-tail indicates that CEI mechanism is very pronounced for the molecular DI and contributes to  $\sim 80\%$  of the total DI yield.

This observation is different from purely classical simulation [23], where CI effect is believed to be overestimated. Our results, however, are consistent with experimental data for Ar atom [20], where ionization potential and laser field parameters are close to our case. The reason is stated as follows: For the intensity of  $0.12 \text{PW}/\text{cm}^2$ , the maximal kinetic energy of the returned electron is  $3.17U_p = 0.85 a.u.$ , still smaller than the ionization energy of  $N_2^+$ . Even with the assistance of the Coulomb focusing [25], it is not easy for the returned electrons to induce too many CI events. Furthermore, such time delay might provide more physics beyond simple rescattering scenario. Recently a statistical thermalization model has been proposed for the nonsequential multiple ionization of atoms in the tunneling regime [26]. This model shows that sharing of excess energy between the tunnelled electron and the bound electrons takes some time, resulting in a time delay on attosecond time scale between recollision and ionization. Our simulation upholds this picture

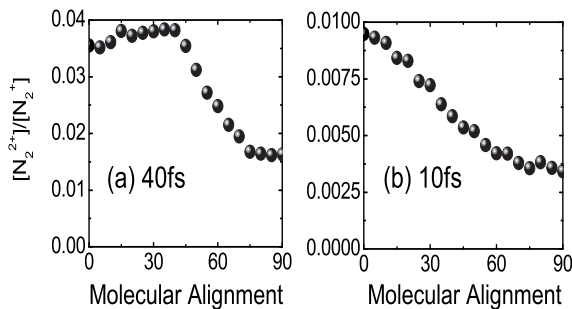


FIG. 5: (color online). The molecular alignment dependence of DI ratios for laser intensity of  $0.15\text{PW}/\text{cm}^2$ .

of attosecond electron thermalization: on upper panel of Fig. 4(c), two bright spots are observed at a similar time delay on subfemtosecond time scale for CI trajectory.

The regular patterns in upper and lower panels of Fig. 4(c) exhibit that the ejection of electrons in the same-hemisphere and opposite-hemisphere emerge alternately with respect to the delayed time. For a time delay of odd half-laser-cycles, two electrons emit in the same direction. In contrast, they emit in the opposite direction for an even half-laser-cycles time delay. In mid of Fig. 4(c), on the other hand, the irregular pattern emerges as the signature of complicated multiple-collision trajectories for DI in the plateau regime. It implies that the trajectories of two electrons entangle with each other before DI ionization occurs and the electrons' motion might be chaotic [27].

When the light intensity is high enough, it has been consensus that DI behavior of atoms is determined by essentially electron physics in the presence of laser field [12, 23]. Good correspondence between our theoretical

calculations and experimental data confirms the validity of the above picture in molecular DI case. In our model, after tunnelling electrons travel much of the time in the intense laser field like a classical object and solely electron collision physics determines the fate of DI of molecules. However, the inherent nuclear degree of freedom of molecule do manifest themselves as the significant alignment effect in our model. To clearly demonstrate it, we calculate the ratios between double and single ionization at different molecular alignment angles. Main results are presented in Fig. 5. It shows that, i) The ratio between DI and single-ionization yield is less for perpendicular molecules than that of parallel molecules; ii) This anisotropy becomes more dramatic for a shorter laser pulse. Further explorations show that molecular alignment also significantly affects the correlated momentum distribution of emitted electrons. Details will be presented elsewhere [28].

In summary, we exploit a semiclassical quasi-static model to achieve insight into the correlated electron dynamics in molecular DI under the relevant experimental conditions, i.e., highly nonperturbative fields with femtosecond or shorter time resolution. Our calculation unveils sub-cycle dynamics behind molecular DI and predicts a significant influence of the molecular alignment on the ratio of double over single ion yield. Because molecular alignment is controllable with present technique [5] the above results can be regarded as our theoretical prediction which may be tested in future experiments.

This work is supported by NNSF of China No.10574019, CAEP Foundation 2006Z0202, and 973 research Project No. 2006CB806000. We thank J. H. Eberly stimulating discussions and are indebted to C. Figueira de Morisson Faria for reading the manuscript carefully and useful suggestions.

- 
- [1] C. Guo, M. Li, J.P. Nibarger, and G.N. Gibson Phys. Rev. A **58**, R4271 (1998).  
 [2] C. Cornaggia and Ph. Hering, Phys. Rev. A **62**, 023403 (2000).  
 [3] A.S. Alnaser et.al., Phys. Rev. Lett. **93**, 113003 (2004)  
 [4] E. Eremina et.al., Phys. Rev. Lett. **92**, 173001 (2004)  
 [5] D. Zeidler, A. Staudte, A.B. Bardon, D.M. Villeneuve, R. Dörner, and P. B. Corkum, Phys. Rev. Lett. **95**, 203003 (2005).  
 [6] See, for example, A. Becker, R. Dörner and R. Moshhammer, J. Phys. B **38**, S753 (2005), and references therein.  
 [7] H. Niikura, et al., Nature (London) **417**, 917 (2002); **421**, 826 (2003).  
 [8] For the treatment of nonsequential double ionization of Helium, see, for example, J.S. Parker et al., J. Phys. B **36**, L393 (2003).  
 [9] A.I. Pegarkov, E. Charron and A. Suzor-Weiner, J. Phys. B **32**, L363(1999).  
 [10] A. Becker and F. H. M. Faisal, J. Phys. B **38**, 1 (2005).  
 [11] J. S. Prauzner-Bechcicki, K. Sacha, B. Eckhardt and J. Zakrzewski, Phys. Rev. A **71**, 033407 (2005).  
 [12] Li-Bin Fu, Jie Liu, Jing Chen, and Shi-Gang Chen Phys. Rev. A **63**, 043416 (2001); Li-Bin Fu, Jie Liu, and Shi-Gang Chen Phys. Rev. A **65**, 021406 (2002).  
 [13] The atomic ADK theory has been extended to diatomic molecules, see, for example, X.M.Tong et al., Phys. Rev. A **66**, 033402 (2002) and I. V. Litvinyuk et al., Phys. Rev. Lett. **90**, 233003 (2003). An explicit analytic expression has also been derived in [28]. However, we found that the employment of atomic ADK formula instead of the complicated molecular ADK formula does not lead to significant discrepancy in calculating the ratios between double and single ionization. So, for simplicity we adopt  $\varpi(t_0) = \frac{4(2I_{p1})^2}{\varepsilon(t_0)} \exp(-\frac{2(2|I_{p1}|)^{3/2}}{3\varepsilon(t_0)})$  in our following calculations.  
 [14] J. Liu and J. Chen, Chin. Phys. Lett. **23** 91 (2006).  
 [15] R. Abrines and I.C. Percival, Proc.Phys.Soc. London **88**, 861 (1966); J.G. Leopold and I.C. Percival, J.Phys.B **12**, 709 (1979).  
 [16] L. Meng, C.O. Reinhold and R.E. Olson, Phys. Rev. A **40**, 3637 (1989).

- [17] G. G. Paulus, W. Becker, W. Nicklich and H. Walther, J. Phys. B: At. Mol. Opt. Phys. **27**, L703 (1994).
- [18] P.J. Ho and J.H. Eberly, Phys. Rev. Lett. **95**, 193002 (2005)
- [19] X. Liu *et al.*, Phys. Rev. Lett. **93**, 263001 (2004).
- [20] B. Feuerstein *et al.*, Phys. Rev. Lett. **87**, 043003 (2001).
- [21] M. Weckenbrock *et al.*, Phys. Rev. Lett. **92**, 213002 (2004).
- [22] P. B. Corkum, Phys. Rev. Lett. **71**, 1994 (1993).
- [23] S.L. Haan, L. Breen, A. Karim, and J.H. Eberly, Phys. Rev. Lett. **97**, 103008 (2006), and references therein.
- [24] Note that these assumptions have been checked by directly tracing the trajectories.
- [25] T. Brabec, M.Yu. Ivanov, and P.B. Corkum, Phys. Rev. A **54**, R2551 (1996).
- [26] X. Liu, C. Figueira de Morisson Faria, W. Becker and P. B. Corkum, J. Phys. B **39**, L305 (2006).
- [27] B. Hu, J. Liu and S.G. Chen, Phys. Lett. A **236**, 533 (1997)
- [28] Y. Li, J. Chen, S.P. Yang, and J. Liu, in preparation.